Photoelectric Charging of Dust Particles in Vacuum

A. A. Sickafoose, J. E. Colwell, M. Horányi, and S. Robertson
Laboratory for Atmospheric and Space Physics, University of Colorado, Boulder, Colorado 80309-0392
(Received 1 March 2000)

Photoelectric charging measurements are presented of dust grains in vacuum for isolated grains and for grains near a photoemissive surface. Isolated grains reach a positive-equilibrium floating potential, dependent upon the work function of the particle, which causes the emitted electrons to be returned. Grains dropped past a photoemitting surface reach a negative floating potential for which the sum of the emitted and collected currents is zero. The particles tested are 90–106 μm in diameter and are composed of Zn, Cu, graphite, and glass.

PACS numbers: 52.25.Zb, 94.10.Nh, 95.30.Wi, 96.50.Dj

Natural and man-made objects in space charge to a floating potential determined by the balance between charging currents in the local plasma environment [1,2]. The dominant currents are the flux of electrons and ions from ambient plasma, electrons created by secondary emission, and photoelectrons. Charging proceeds until the sum of the charging currents is zero and the object has reached an equilibrium floating potential. The charging of objects in interplanetary space is typically dominated by photoelectric emission. In this situation, the object obtains a positive equilibrium floating potential at which nearly all of the photoelectrons are returned to the surface. This potential is altered only slightly by the small flux of solar wind electrons.

For objects approaching centimeter scale and larger, the local plasma environment is dominated by photoelectrons which create a sheath at the surface. Electron energy analyzers have observed low energy photoelectrons which originate at spacecraft and are returned to the surface by the sheath potential [3]. These analyzers also see ambient plasma particles accelerated toward spacecraft by this potential [4]. For smaller objects such as dust grains, the particle size is small with respect to the Debye length and a photoelectron sheath is not created. Dust on the surface of larger objects such as the Moon [5], Mercury [6], asteroids [7], and the moons of Mars may be charged, levitated, and transported in the sheath of the parent object [8]. For example, dust grains suspended above the lunar surface have been observed on multiple occasions [9].

Photoelectric emission will cause an isolated grain in vacuum to attain a positive charge. For an illumination spectrum having a short wavelength cutoff λ, and a particle with a photoelectric work function W, the floating potential is $V = (hc/\lambda - W)/e$ where e is the elementary charge. The charge on the grain is determined by $Q = CV$ where C is the capacitance of the grain. For spherical grains of radius r, $C = 4\pi\varepsilon_0 r$ and the charge is

$$Q = 4\pi\varepsilon_0 r(hc/\lambda - W)/e\,. \quad (1)$$

Grains at a sufficient distance above the sheath may charge positively by photoemission, and it is for these grains that the electric force above the parent body will be in the direction opposite to gravity. On the other hand, grains near a photoemitting surface are more likely to be charged negatively by the sheath electrons than by their own photoemission.

We have performed experiments to investigate the charging of dust particles by their own photoemission current and by photoemission from an adjacent surface. The dust particles are 90–106 μm in diameter and are composed of zinc, copper, graphite, and glass. The experiments are performed at one end of a cylindrical aluminum vacuum chamber 30 cm in diameter (Fig. 1) pumped to a base pressure of 4×10^{-7} Torr [10]. At the top of the chamber is a dust dropper and below it is a Faraday cup that receives the dust particles. The dust dropper consists of a thin metal disk with a small central hole and is agitated by an electromagnet. The Faraday cup is attached to a sensitive electrometer and the height of the output pulse indicates the charge on the grain [10]. Signals from multiple grains are excluded from the analysis. The rms electrical noise corresponds to a charge of approximately $(5 \times 10^3)e$, and the threshold for detection is set at $\pm 2 \times 10^4 e$ to avoid false detections.

Photoelectron emission of $\sim$20 μm is induced by a 1 kW Hg-Xe arc lamp. The light is collimated by a lens

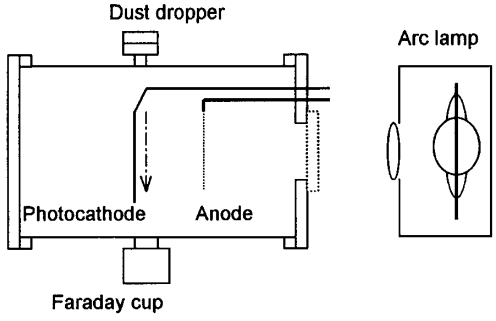

FIG. 1. Schematic diagram of the experiment. The anode is used in characterizing the photoemission from the surface of the zirconium plate and is removed during dust charging measurements.

 0031-9007/00/84(26)/6034(4)$15.00

and directed through a quartz window into the vacuum system. The photocathode is a 12.5-cm diameter zirconium foil plate. Zirconium has nearly the lowest work function (4.05 eV) of elements that do not react with air [11]. There is also an anode, composed of a highly transparent, 15-cm square, nickel wire grid which may be electrically biased.

The electron sheath above the cathode of a vacuum tube has received extensive analysis [12]. The emitted electrons have a single-sided Maxwell-Boltzmann distribution with a mean energy of order 0.1 eV determined by the cathode temperature. For a laboratory generated photoelectron sheath, however, the energy distribution has a width of several eV and has a well-defined high energy cutoff determined by the work function of the material and the short-wavelength cutoff of the spectrum. The sheath potential profile can be found by simultaneously solving Poisson's equation and the Vlasov equation. Solutions have been given for several model electron velocity distribution functions [5,13].

In our experiment, the photoelectron energy distribution perpendicular to the photocathode is determined by retarding potential analysis. The photocathode is swept in voltage and the emitted current is measured. The anode mesh is spaced 2.5 cm from, and parallel to, the photocathode and is held at -4.5 V to prevent collection of electrons emitted from the walls of the chamber (see Fig. 1). The Zr plate is illuminated in a central region $\sim$10 cm in diameter to minimize electron losses from the edge. Figure 2(a) shows the photocathode current as a function of bias potential and Fig. 2(b) shows the derivative of this curve which gives the electron energy distribution perpendicular to the plate. For these data, the photocurrent was decreased to 2 μA to reduce space charge effects that perturb the applied potential. The absence of a reverse current in Fig. 2(a) indicates negligible emission by surfaces other than the photocathode. The small "wings" on the distribution are probably due to small patches of material having a different work function than zirconium.

A modified kappa function [14] fit to the energy distribution has intercepts that are separated in energy by 1.96 eV (excluding the wings). This is approximately the difference between the maximum photon energy (6.03 eV) and the tabulated work function of Zr (4.05 eV). The peak of the energy distribution indicates a mean energy of emission of $\sim$1.3 eV, which corresponds to a mean emission velocity of 6.8×10^5 m/s. For an average photoemission of 20 μA, the density of photoelectrons immediately above the surface is 2.3×10^4 cm^{-3}. This density is doubled when the photocathode is at the floating potential and the emitted electrons are returned to the surface. The Debye length in this case is approximately 4 cm.

The charge due to photoemission on grains of Zn, Cu, and graphite was measured by exposing the particles to ultraviolet illumination. For these experiments, the photocathode and anode are removed from the chamber. In the absence of illumination, there are no trigger events, indicating that the initial charge is less than the threshold of $\pm 2 \times 10^4$ e. Data were taken for 100 particles and plotted as a histogram in Figs. 3(a)–3(c). The mean measured charge is positive with a value of 5.3 ($\pm$1.6) $\times 10^4$ e for zinc grains, 5.0 ($\pm$1.0) $\times 10^4$ e for copper grains, and 4.1 ($\pm$1.0) $\times 10^4$ e for graphite grains. The capacitance for spherical grains with a mean radius of 49 μm (the middle of our size range) is 5.4 fF which indicates that the charge should be $\sim 3.4 \times 10^4$ e per volt of charging potential. The expected particle potential is given by $V = (hc/\lambda - W)/e$, where the maximum photon energy from the light source $hc/\lambda \approx 6.03$ eV. The tabulated work functions are $W = 4.33$ eV for zinc, $W = 4.65$ eV for copper, and $W = 5.0$ eV for graphite [11]. A plot of

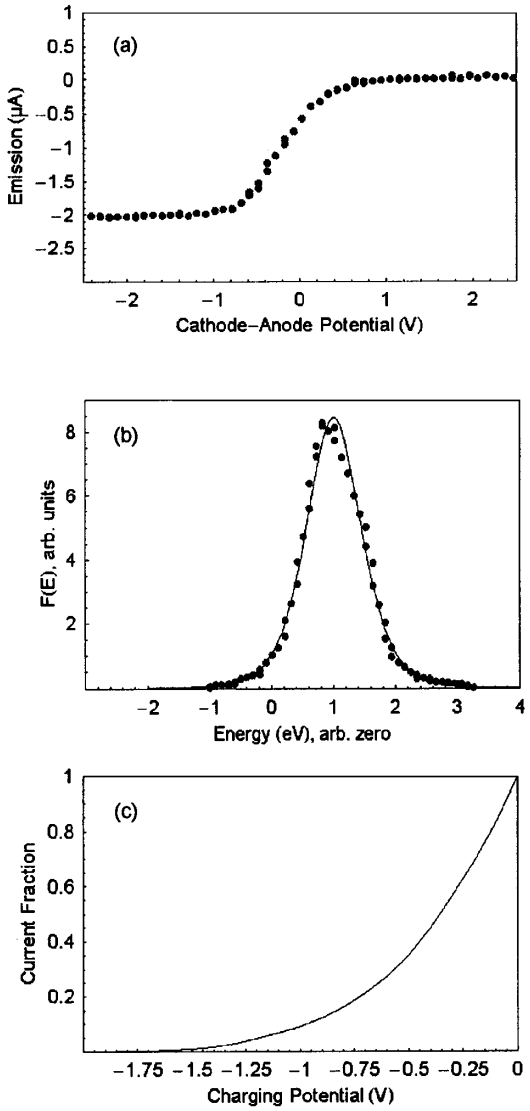

FIG. 2. Current-voltage characteristics of the zirconium photocathode. (b) The electron energy distribution perpendicular to the zirconium photocathode, determined from the derivative of the data in (a). The solid line is a least-squares kappa function fit to the data, with $\kappa = 2.31$ and $k_B T = 1.42$ eV. (c) Fraction of the current to the grain as a function of the grain potential.

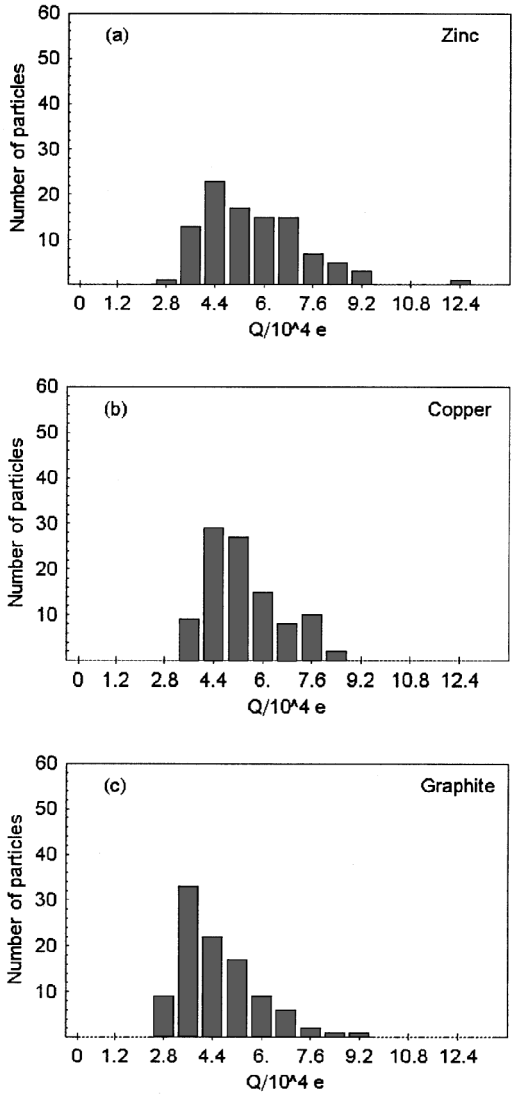

FIG. 3. Charge distributions for 100 grains of (a) zinc, (b) copper, and (c) graphite dropped through the UV beam. The bin size is 0.8×10^4 e with zero labeled for reference.

measured charge as a function of V, Fig. 4 shows that the charge is approximately the value obtained from Eq. (1). The short wavelength cutoff and the work function could not be varied over a sufficiently wide range to verify that the experimental line has the proper slope. In addition, there is a systematic error in the mean arising from rejecting data below the threshold. This error results in overestimation of charge for materials having charge near the threshold.

In the second set of experiments, the charge on grains dropped through the photoelectron sheath was measured for grains of zinc, copper, and graphite. The grains fell less than 2 cm from the surface of the photoemitter. The grain charging time is of the order of 0.1 ms and is much shorter than the sheath transit time of 100 ms. The grains are expected to charge to the negative potential determined by collection of electrons from the sheath, and the charging

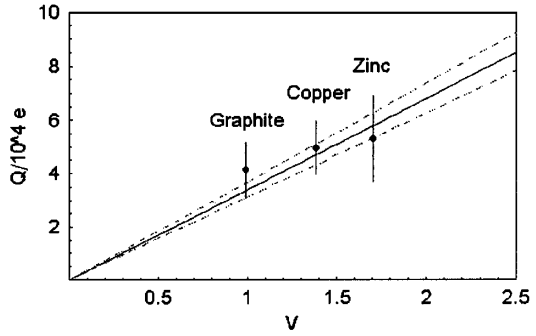

FIG. 4. The mean measured charge for zinc, copper, and graphite particles exposed to UV illumination as a function of the particle potential, $V = (hc/\lambda - W)$. The slope of the solid line is the capacitance of an isolated spherical grain, $C = Q/V$, for $r = 49$ μm. The dashed lines represent the capacitance for the upper and lower limits of the particle size range, $r = 45$ μm and $r = 53$ μm. The error bars are the standard deviation of the mean.

does not depend on particle composition. The mean charge measured on zinc (Fig. 5) is -4.3 $(\pm 0.9) \times 10^4$ e. Data for copper and graphite are not significantly different. This charge corresponds to a potential of -1.26 (± 0.3) V.

For a monoenergetic electron distribution of energy E, the electron current collected by a grain with a potential V is $I = J_0 A[1 + eV/E]$ for $eV > -E$, where J_0 is the current density to a surface at zero potential and A is the surface area of the grain. For a distribution of electrons, $F(E)$, the collected current is

$$I(V) = J_0 A \int_{-eV}^{K} F(E)\left[1 + \frac{eV}{E}\right] dE, \qquad eV > -E \tag{2}$$

for a maximum electron energy K. The current collected by the grain as a function of its potential, using the measured energy distribution function plotted in Fig. 2(b), is shown in Fig. 2(c). For the spectrum of illumination in our experiment, the photoelectron yield from a photocathode of Zn was determined to be 0.12 that of Zr. Since

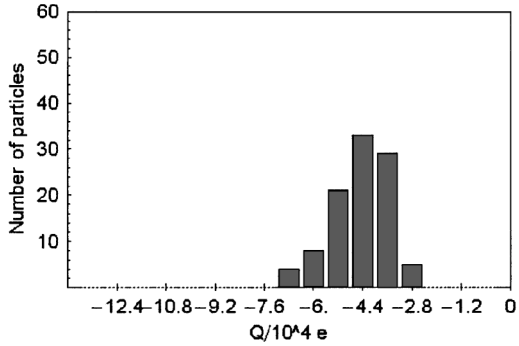

FIG. 5. Measured charge distribution for 100 particles of zinc dust dropped through the photoelectron sheath. The bin size is 0.8×10^4 e, and zero is labeled for reference.

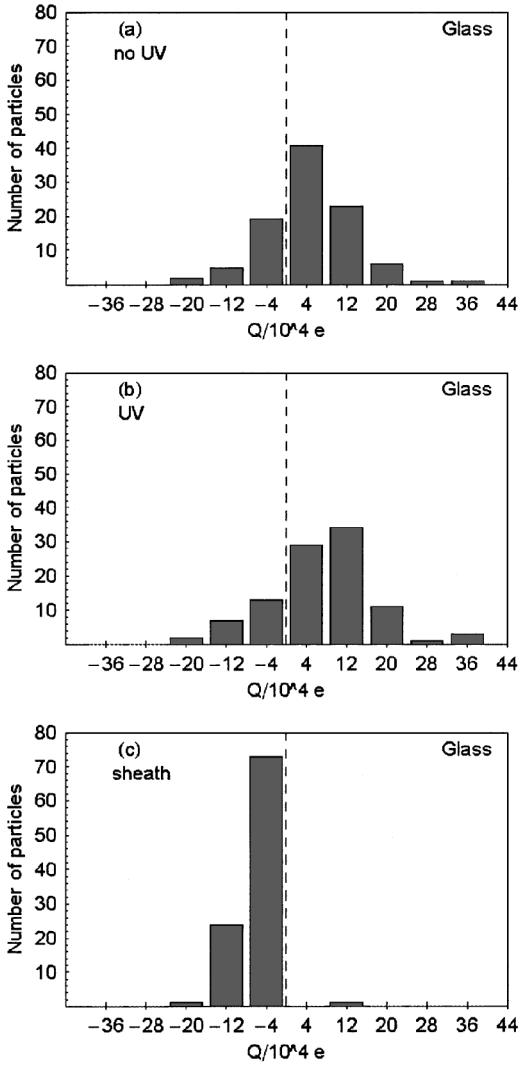

FIG. 6. Measured charge distributions for (a) 100 particles of glass dropped through the chamber with no illumination, (b) 100 particles of glass dropped through the UV beam, and (c) 100 particles of glass dropped through the photoelectron sheath. The bin size is 8.0×10^4 e, an order of magnitude larger than in the previous charge plots.

the current density immediately above the photocathode is doubled by the return of the electrons to the surface, the grains should charge to the potential at which 0.06 of the current from the surface is collected. This occurs at a charging potential of -1.17 V, which compares favorably with the potential of -1.26 (± 0.3) V calculated from the measured charge.

The data for glass, a nonconductor, showed different behavior from that of the conducting materials. A charge histogram for glass obtained with no illumination, Fig. 6(a), show that most grains leave the dust dropper with an initial charge above the threshold for detection. There is a broad charge distribution centered at 4.0×10^4 e with an rms value 10.8×10^4 e corresponding to an rms charging voltage of 3.2 V. This charge occurs in the dust dropper and is apparently triboelectric. The charge distribution for glass obtained with UV illumination is shown in Fig. 6(b). This distribution is more positive, with an average charge of 7.0×10^4 e and a standard deviation of 10.8×10^4 e. The relatively small shift in the center of the distribution results from photoelectron emission with a yield that is too low for an equilibrium charge to be obtained. The data for glass particles dropped through the photoelectron sheath are shown in Fig. 6(c). This distribution has an average of -5.9×10^4 e with a standard deviation of 4.1×10^4 e. Positively charged particles are absent from this distribution because they are neutralized by electrons collected from the sheath. The average charge is more negative than that of the conducting grains because many particles have a negative initial triboelectric charge that is retained because of the low photoelectric yield of glass.

The authors thank Bob Walch, University of Northern Colorado, for initial development of the apparatus. A. S. and J. C. acknowledge support from the National Aeronautics and Space Administration (Microgravity), and S. R. and M. H. acknowledge support from the Department of Energy (Fusion Energy Sciences).

[1] E. C. Whipple, Rep. Prog. Phys. **44**, 1197 (1981).
[2] C. K. Goertz, Rev. Geophys. **27**, 271 (1989).
[3] E. C. Whipple, Jr., J. Geophys. Res. **81**, 815 (1976).
[4] S. E. DeForest, J. Geophys. Res. **77**, 651 (1972).
[5] S. F. Singer and E. H. Walker, Icarus **1**, 112 (1962).
[6] R. Grard, Planet. Space Sci. **45**, 67 (1997).
[7] P. Lee, Icarus **124**, 181 (1996).
[8] T. Nitter *et al.*, IEEE Trans. Plasma Sci. **22**, 159 (1994); T. Nitter and O. Havnes, Earth Moon Planets **56**, 7 (1992).
[9] J. J. Rennilson and D. R. Criswell, Moon **10**, 121 (1974); H. A. Zook and J. E. McCoy, Geophys. Res. Lett. **18**, 2117 (1991); H. A. Zook, A. E. Potter, and B. L. Cooper, Lunar Planet. Sci. Conf. **26**, 1577 (1995).
[10] B. Walch, M. Horányi, and S. Robertson, Phys. Rev. Lett. **75**, 838 (1995).
[11] H. B. Michaelson, J. Appl. Phys. **48**, 4729 (1977).
[12] *The Collected Works of Irving Langmuir,* edited by C. G. Suits (Pergamon, New York, 1961), Vols. 3 and 4.
[13] E. Walbridge, J. Geophys. Res. **78**, 3668 (1973); R. J. L. Grard and J. K. E. Tunaley, J. Geophys. Res. **76**, 2498 (1971).
[14] D. A. Mendis and M. Rosenberg, Annu. Rev. Astron. Astrophys. **32**, 419 (1994).